

C P \rightarrow V isolating A sym m etries in B^0 ! +
M illion $B\bar{B}$ Pairs

K .Abe,¹⁰ K .Abe,⁴⁶ N .Abe,⁴⁹ I .Adachi,¹⁰ H .Aihara,⁴⁸ M .Akatsu,²⁴ Y .Asano,⁵³
 T .Aso,⁵² V .Aulchenko,² T .Aushev,¹⁴ T .A ziz,⁴⁴ S .Bahinipati,⁶ A .M .Bakich,⁴³
 Y .Ban,³⁶ M .Barbero,⁹ A .Bay,²⁰ I .Bedny,² U .Bitenc,¹⁵ I .Bizjak,¹⁵ S .Blyth,²⁹
 A .Bondar,² A .Bozek,³⁰ M .Bracko,^{22,15} J .Brodzicka,³⁰ T .E .Browder,⁹ M .C .Chang,²⁹
 P .Chang,²⁹ Y .Chao,²⁹ A .Chen,²⁶ K .F .Chen,²⁹ W .T .Chen,²⁶ B .G .Cheon,⁴
 R .Chistov,¹⁴ S .K .Choi,⁸ Y .Choi,⁴² Y .K .Choi,⁴² A .Chuvikov,³⁷ S .Cole,⁴³
 M .Danilov,¹⁴ M .Dash,⁵⁵ L .Y .Dong,¹² R .Dowd,²³ J .Dragic,²³ A .Dnutskoy,⁶
 S .Eidelman,² Y .Enari,²⁴ D .Epifanov,² C .W .Everton,²³ F .Fang,⁹ S .Fratina,¹⁵
 H .Fuji,¹⁰ N .Gabyshev,² A .Gamash,³⁷ T .Gershon,¹⁰ A .Go,²⁶ G .Gokhroo,⁴⁴
 B .Golob,^{21,15} M .Grosse Perdekamp,³⁸ H .Guler,⁹ J .Haba,¹⁰ F .H anda,⁴⁷ K .Hara,¹⁰
 T .Hara,³⁴ N .C .Hastings,¹⁰ K .Hasuko,³⁸ K .Hayasaka,²⁴ H .Hayashii,²⁵ M .Hazumi,¹⁰
 E .M .Heenan,²³ I .Higuchi,⁴⁷ T .Higuchi,¹⁰ L .Hinz,²⁰ T .Hojo,³⁴ T .Hokuue,²⁴
 Y .Hoshi,⁴⁶ K .Hoshina,⁵¹ S .Hou,²⁶ W .S .Hou,²⁹ Y .B .Hsiung,²⁹ H .C .Huang,²⁹
 T .Igaki,²⁴ Y .Igarashi,¹⁰ T .Iijima,²⁴ A .Imoto,²⁵ K .Inami,²⁴ A .Ishikawa,¹⁰ H .Ishino,⁴⁹
 K .Itoh,⁴⁸ R .Itoh,¹⁰ M .Iwamoto,³ M .Iwasaki,⁴⁸ Y .Iwasaki,¹⁰ R .Kagan,¹⁴ H .Kakuno,⁴⁸
 J .H .Kang,⁵⁶ J .S .Kang,¹⁷ P .Kapusta,³⁰ S .U .Kataoka,²⁵ N .Katayama,¹⁰ H .Kawai,³
 H .Kawai,⁴⁸ Y .Kawakami,²⁴ N .Kawamura,¹ T .Kawasaki,³² N .Kent,⁹ H .R .Khan,⁴⁹
 A .Kabayashi,⁴⁹ H .Kichimi,¹⁰ H .J .Kim,¹⁹ H .O .Kim,⁴² Hyunwoo Kim,¹⁷ J .H .Kim,⁴²
 S .K .Kim,⁴¹ T .H .Kim,⁵⁶ K .Kinoshita,⁶ P .Oppenburg,¹⁰ S .Korpar,^{22,15} P .Krizan,^{21,15}
 P .Krokovny,² R .Kulasiri,⁶ C .C .Kuo,²⁶ H .Kurashiro,⁴⁹ E .Kurihara,³ A .Kusaka,⁴⁸
 A .Kuzmin,² Y .J .Kwon,⁵⁶ J .S .Lange,⁷ G .Leder,¹³ S .E .Lee,⁴¹ S .H .Lee,⁴¹
 Y .J .Lee,²⁹ T .Lesiak,³⁰ J .Li,⁴⁰ A .Limosani,²³ S .W .Lin,²⁹ D .Liventsev,¹⁴
 J .Madnauthon,¹³ G .Majumder,⁴⁴ F .Mandl,¹³ D .Marlow,³⁷ T .Matsuishi,²⁴
 H .Matsumoto,³² S .Matsumoto,⁵ T .Matsumoto,⁵⁰ A .M atyja,³⁰ Y .M ikami,⁴⁷
 W .Mitaro,¹³ K .Miyabayashi,²⁵ Y .Miyabayashi,²⁴ H .Miyake,³⁴ H .Miyata,³² R .Mizuk,¹⁴
 D .Mohapatra,⁵⁵ G .R .Moloney,²³ G .F .Moorhead,²³ T .Mori,⁴⁹ A .Murakami,³⁹
 T .Nagamine,⁴⁷ Y .Nagasaki,¹¹ T .Nakadaira,⁴⁸ I .Nakamura,¹⁰ E .Nakano,³³ M .Nakao,¹⁰
 H .Nakazawa,¹⁰ Z .Natkaniec,³⁰ K .Neichi,⁴⁶ S .Nishida,¹⁰ O .Nishio,⁵¹ S .Noguchi,²⁵
 T .Nozaki,¹⁰ A .Ogawa,³⁸ S .Ogawa,⁴⁵ T .Ohshima,²⁴ T .Okabe,²⁴ S .Okuno,¹⁶
 S .L .Olson,⁹ Y .Onuki,³² W .Ostrowicz,³⁰ H .Ozaki,¹⁰ P .Pakhlov,¹⁴ H .Palka,³⁰
 C .W .Park,⁴² H .Park,¹⁹ K .S .Park,⁴² N .Parslow,⁴³ L .S .Peak,⁴³ M .Pernicka,¹³
 J .P .Perroud,²⁰ M .Peters,⁹ L .E .Piilonen,⁵⁵ A .Poluektov,² F .J .Ronga,¹⁰ N .Root,²
 M .Rozanska,³⁰ H .Sagawa,¹⁰ M .Saigo,⁴⁷ S .Saitoh,¹⁰ Y .Sakai,¹⁰ H .Sakamoto,¹⁸
 T .R .Sarangi,¹⁰ M .Satapathy,⁵⁴ N .Sato,²⁴ O .Schneider,²⁰ J .Schumann,²⁹ C .Schwanda,¹³
 A .J .Schwartz,⁶ T .Seki,⁵⁰ S .Semnov,¹⁴ K .Senyo,²⁴ Y .Settai,⁵ R .Seuster,⁹
 M .E .Sevior,²³ T .Shibata,³² H .Shibuya,⁴⁵ B .Shwartz,² V .Sidorov,² V .Siegle,³⁸
 J .B .Singh,³⁵ A .Somov,⁶ N .Soni,³⁵ R .Stamen,¹⁰ S .Stanic,⁵³, M .Staric,¹⁵ A .Sugi,²⁴
 A .Sugiyama,³⁹ K .Sumisawa,³⁴ T .Sumiyoshi,⁵⁰ S .Suzuki,³⁹ S .Y .Suzuki,¹⁰ O .Tajima,¹⁰
 F .Takasaki,¹⁰ K .Tamaai,¹⁰ N .Tamura,³² K .Tanabe,⁴⁸ M .Tanaka,¹⁰ G .N .Taylor,²³

Y .Teram oto,³³ X .C .T ian,³⁶ S .Tokuda,²⁴ S .N .Tovey,²³ K .Trabelsi,⁹ T .T suboyam a,¹⁰
T .T suka m oto,¹⁰ K .U chida,⁹ S .U ehara,¹⁰ T .U glow,¹⁴ K .U eno,²⁹ Y .Unno,³ S .Uno,¹⁰
Y .U shiroda,¹⁰ G .Varner,⁹ K .E .Varvell,⁴³ S .V illa,²⁰ C .C .W ang,²⁹ C .H .W ang,²⁸
J .G .W ang,⁵⁵ M .Z .W ang,²⁹ M .W atanabe,³² Y .W atanabe,⁴⁹ L .W idhalm ,¹³
Q .L .X ie,¹² B .D .Yabsley,⁵⁵ A .Yam aguchi,⁴⁷ H .Yam am oto,⁴⁷ S .Yam am oto,⁵⁰
T .Yam anaka,³⁴ Y .Yam ashita,³¹ M .Yam audi,¹⁰ H eyoung Yang,⁴¹ P .Yeh,²⁹ J .Y ing,³⁶
K .Yoshida,²⁴ Y .Yuan,¹² Y .Yusa,⁴⁷ H .Yuta,¹ S .L .Zang,¹² C .C .Zhang,¹² J .Zhang,¹⁰
L .M .Zhang,⁴⁰ Z .P .Zhang,⁴⁰ V .Zhilich,² T .Ziegler,³⁷ D .Zontar,^{21,15} and D .Zurcher²⁰

(The Belle Collaboration)

¹Aom ori University, Aom ori

²Budker Institute of Nuclear Physics, Novosibirsk

³Chiba University, Chiba

⁴Chonnam National University, Kwangju

⁵Chuo University, Tokyo

⁶University of Cincinnati, Cincinnati, Ohio 45221

⁷University of Frankfurt, Frankfurt

⁸Gyeongsang National University, Chinju

⁹University of Hawaii, Honolulu, Hawaii 96822

¹⁰High Energy Accelerator Research Organization (KEK), Tsukuba

¹¹Hiroshima Institute of Technology, Hiroshima

¹²Institute of High Energy Physics,

Chinese Academy of Sciences, Beijing

¹³Institute of High Energy Physics, Vienna

¹⁴Institute for Theoretical and Experimental Physics, Moscow

¹⁵J .Stefan Institute, Ljubljana

¹⁶Kanagawa University, Yokohama

¹⁷Korea University, Seoul

¹⁸Kyoto University, Kyoto

¹⁹Kyungpook National University, Taegu

²⁰Swiss Federal Institute of Technology of Lausanne, EPFL, Lausanne

²¹University of Ljubljana, Ljubljana

²²University of Maribor, Maribor

²³University of Melbourne, Victoria

²⁴Nagoya University, Nagoya

²⁵Nara Women's University, Nara

²⁶National Central University, Chung-li

²⁷National Kaohsiung Normal University, Kaohsiung

²⁸National United University, Miao Li

²⁹Department of Physics, National Taiwan University, Taipei

³⁰H .Niewodniczanski Institute of Nuclear Physics, Krakow

³¹Nihon Dental College, Niigata

³²Niigata University, Niigata

³³Osaka City University, Osaka

³⁴Osaka University, Osaka

³⁵Panjab University, Chandigarh

³⁶Peking University, Beijing

- ³⁷Princeton University, Princeton, New Jersey 08545
³⁸RIKEN BNL Research Center, Upton, New York 11973
³⁹Saga University, Saga
⁴⁰University of Science and Technology of China, Hefei
⁴¹Seoul National University, Seoul
⁴²Sungkyunkwan University, Suwon
⁴³University of Sydney, Sydney NSW
⁴⁴Tata Institute of Fundamental Research, Bom bay
⁴⁵Toho University, Funabashi
⁴⁶Tohoku Gakuin University, Tagajo
⁴⁷Tohoku University, Sendai
⁴⁸Department of Physics, University of Tokyo, Tokyo
⁴⁹Tokyo Institute of Technology, Tokyo
⁵⁰Tokyo Metropolitan University, Tokyo
⁵¹Tokyo University of Agriculture and Technology, Tokyo
⁵²Toyama National College of Maritime Technology, Toyama
⁵³University of Tsukuba, Tsukuba
⁵⁴Utkal University, Bhubaneswar
⁵⁵Virginia Polytechnic Institute and State University, Blacksburg, Virginia 24061
⁵⁶Yonsei University, Seoul
- (Dated: January 27, 2020)

Abstract

We present a new measurement of the time-dependent CP-violating parameters in $B^0 \rightarrow B^+ \pi^-$ decays using a 253 fb^{-1} data sample that contains $275 \times 10^6 B\bar{B}$ pairs collected with the Belle detector at the KEKB asymmetric-energy e^+e^- collider operating at the $(4S)$ resonance. We reconstruct one neutral B meson as a B^+ CP eigenstate and identify the flavor of the accompanying B meson from its decay products. We find $666 \pm 43 B^0 \rightarrow B^+ \pi^-$ events and perform an unbinned maximum likelihood fit to the distribution of the proper time differences between the two B meson decays. The fit yields the CP-violating parameters: $S = -0.67 \pm 0.16(\text{stat}) \pm 0.06(\text{syst})$ and $A = +0.56 \pm 0.12(\text{stat}) \pm 0.06(\text{syst})$. Large direct CP violation is observed with a significance greater than 4 standard deviations for any S value. Using isospin relations, we obtain 95.4% confidence intervals for the CKM angle β of $0^\circ < \beta < 19^\circ$ and $71^\circ < \beta < 180^\circ$.

PACS numbers: 11.30.Er, 12.15.Hh, 13.25.Hw, 14.40.Nd

on leave from Nova Gorica Polytechnic, Nova Gorica

One of the unresolved mysteries in particle physics is the origin of CP violation. Kobayashi and Maskawa (KM) pointed out in 1973 that CP violation can be incorporated as an irreducible complex phase in the weak-interaction quark mixing matrix in the standard model (SM) framework [1]. Recent measurements of one of the CP-violating parameters, $\sin 2\beta_1$, by Belle [2, 3] and BABAR [4] support the KM model. Measurements of other CP-violating parameters provide important additional tests of the model. In this Letter, we describe a measurement of CP-violating asymmetries in the $B^0 \rightarrow B^0 \bar{B}^0$ decay [5] that is sensitive to the parameter β_2 (or γ).

The KM model predicts CP-violating asymmetries in the time-dependent rates of neutral B meson decays to a common CP eigenstate [6]. In the decay chain of $(4S) \rightarrow B^0 \bar{B}^0 \rightarrow (f_{tag})^+$, one of the neutral B mesons decays into a CP eigenstate f_{tag}^+ at time t and the other decays at time t_{tag} to a final state f_{tag} that distinguishes the flavor of the B meson. The time-dependent decay rate is given by

$$P^q(t) = \frac{e^{j t \frac{\Delta m}{m_d}}}{4} [1 + q f_S \sin(m_d t) + A \cos(m_d t) g]; \quad (1)$$

where $t = t - t_{tag}$, m_d is the mass difference between the two neutral B mass eigenstates, and q is the b-flavor charge, i.e., $q = +1 (-1)$ for $f_{tag} = B^0 (\bar{B}^0)$. We measure S and A , which are mixing-induced and direct CP-violating parameters, respectively. In the case where only a $b \rightarrow u$ tree transition contributes to the decay $B^0 \rightarrow B^0 \bar{B}^0$, we would have $S = \sin 2\beta_2$ and $A = 0$. Because of possible contributions from gluonic $b \rightarrow d$ penguin transitions that have a different weak phase and additional strong phases, S may deviate from $\sin 2\beta_2$, and direct CP violation, $A \neq 0$, may occur. A previous measurement by the Belle Collaboration based on a 140 fb^{-1} data sample indicated large S and A values [7], while no significant CP asymmetry was observed by the BABAR Collaboration [8]. It is therefore important to measure the CP-violating parameters with larger statistics.

The measurement in this Letter is based on a 253 fb^{-1} data sample containing $275 \times 10^6 B\bar{B}$ pairs collected with the Belle detector at the KEKB e⁺e⁻ asymmetric-energy (3.5 on 8 GeV) collider [9] operating at the $(4S)$ resonance. The $(4S)$ is produced with a Lorentz boost factor of $\gamma = 0.425$ along the z axis, which is antiparallel to the positron beam direction. Since the two B mesons are produced nearly at rest in the $(4S)$ center-of-mass system (CM S), the decay time difference t is determined from the distance between the two B meson decay positions along the z-direction (z): $t = z/c$, where c is the velocity of light.

The Belle detector [10] is a large-solid-angle magnetic spectrometer that consists of a silicon vertex detector (SVD), a 50-layer central drift chamber (CDC), an array of aerogel threshold Cherenkov counters (ACC), a barrel-like arrangement of time-of-light scintillation counters (TOF), and an electromagnetic calorimeter (ECL) comprised of CsI(Tl) crystals located inside a superconducting solenoid coil that provides a 1.5 T magnetic field. An iron flux-return located outside of the coil is instrumented to detect K_L^0 mesons and to identify muons (KLM). Two different inner detector configurations were used. A sample containing $152 \times 10^6 B\bar{B}$ pairs (Set I) was collected with a 2.0 cm radius beam pipe and a 3-layer silicon vertex detector (SVD-I); a sample with $123 \times 10^6 B\bar{B}$ pairs (Set II) was collected with a 1.5 cm radius beam pipe, a 4-layer silicon detector (SVD-II), and a small-cell inner drift chamber [11].

We reconstruct $B^0 \rightarrow B^0 \bar{B}^0$ candidates using oppositely charged track pairs that are

positively identified as pions by combining information from the ACC and the CDC dE/dx measurements. The pion detection efficiency is 90%, and 11% of kaons are misidentified as pions. We select B^- meson candidates using the energy difference $E - E_B - E_{beam}$ and the beam-energy constrained mass $M_{bc} = \sqrt{(E_{beam})^2 - (p_B)^2}$, where E_{beam} is the CMS beam-energy, and E_B and p_B are the CMS energy and momentum of the B^- candidate. We define the signal region as $5.271 \text{ GeV}/c^2 < M_{bc} < 5.287 \text{ GeV}/c^2$ and $|E| < 0.064 \text{ GeV}$, which corresponds to 3 standard deviations (σ) from the central values.

We identify the flavor of the accompanying B^- meson from inclusive properties of particles that are not associated with the reconstructed $B^0 \rightarrow \pi^+ \pi^-$ decay. We use r defined in Eq. (1) and r to represent the tagging information. The parameter r is an event-by-event, Monte Carlo (MC) determined flavor-tagging dilution factor that ranges from $r = 0$ for no flavor discrimination to $r = 1$ for unambiguous flavor assignment. It is used only to sort data into six r intervals. The wrong tag fractions for the six r intervals, w_1 ($l = 1; 6$), and the differences between B^0 and \bar{B}^0 decays, w_{1l} , are determined from data [12, 13].

To suppress the continuum background ($e^+ e^- \rightarrow q\bar{q}; q = u; d; s; c$), we form signal and background likelihood functions, L_S and L_{BG} , from the event topology and the B^- flight direction in the CMS with respect to the z axis, and impose requirements on the likelihood ratio $LR = L_S/(L_S + L_{BG})$ for the candidate events. We determine the LR threshold by optimizing the expected sensitivity and require $LR > 0.86$ for all r intervals. We also include additional candidate events with lower likelihood ratio thresholds (0.50, 0.45, 0.45, 0.45, and 0.20) for the six r intervals, respectively. The thresholds are changed with r since the separation of the continuum background from B^- signal depends on r . We accept candidate events in 12 distinct regions of the $LR-r$ plane.

For the data in Set I, we reconstruct decay vertex positions of the two B^- mesons using the method described in Ref. [7]. The positions are formed from charged tracks having SVD hits with a constraint from the interaction point (IP) profile. This profile is determined run-by-run from hadronic events and smeared in the r -plane, i.e. the plane perpendicular to the beam direction, to account for the B^- flight path of 22 m. This constraint enables us to reconstruct the decay vertices even with a single track. For the data in Set II, this vertex algorithm produces a larger outlier fraction for vertices reconstructed with a single track. We reduce this by imposing more stringent SVD-II hit pattern requirements on the tracks [13].

We extract 2,820 signal candidates by applying the above cuts to the data sample. Figure 1 shows the E distributions for the events with (a) $LR > 0.86$ and (b) $LR < 0.86$ in the M_{bc} signal region. The $B^0 \rightarrow \pi^+ \pi^-$ signal yield is determined from an unbinned two-dimensional maximum likelihood fit to the $E-M_{bc}$ distribution in the range of $5.20 \text{ GeV}/c^2 < M_{bc} < 5.30 \text{ GeV}/c^2$ and $0.3 \text{ GeV} < E < +0.5 \text{ GeV}$ with a Gaussian signal function plus contributions from misidentified $B^0 \rightarrow K^+ K^-$ events, the continuum background, and three-body B^- decays. The continuum background shapes in E and M_{bc} are described by a first order polynomial and an ARGUS function [14], respectively. For the three-body B^- decay background shape, we employ a smoothed two-dimensional histogram obtained from a large MC sample. The fit to the subset with $LR > 0.86$ yields 415 π^+ events and 154 K^+ events in the signal region, where the errors are statistical only. The K^+ contamination is consistent with the $K^+ \rightarrow \pi^+$ misidentification probability, which is measured independently. Extrapolating from the size of the continuum background in this fit, we expect 315 π^+ continuum events in the signal region. For $LR < 0.86$, we apply the same procedure used in the previous publication [7]. We find 251 π^+ ,

93 B^0 and 1,592 continuum events in the signal region. The contribution from three-body B^- decays is negligibly small in the signal region.

We determine S and A_{CP} by applying an unbinned maximum likelihood fit to the distribution of proper time difference t . The probability density function (PDF) for the signal events is given in Eq. (1) modified to incorporate the effect of incorrect flavor assignment w_1 and w_1 . The distribution is convolved with the proper time interval resolution function $R_{sig}(t)$ in order to take into account the finite position resolution, the shift of vertex position of f_{tag} due to secondary tracks originating from charmed particle decays, and the smearing due to the kinematic approximation used to convert z to t [13, 16]. The PDF for $B^0 \rightarrow K^+ K^-$ is $P_K^q(t; w_1, w_1) = (1-f_{B^0})e^{-\frac{1}{2}t^2} f_1(q w_1 + q(1-2w_1)A_K^e \cos(m_d t))g$. We use $A_K^e = (A_K + A_{\pi})/(1 + A_K A_{\pi})$, where $A_K = 0.109 \pm 0.019$ is the direct CP-violating parameter in $B^0 \rightarrow K^+ K^-$ decays [15], and A_{π} is the difference in the product of the pion efficiency and kaon misidentification probability between $K^+(K^-)$ and $K^-(K^+)$ divided by their sum [17]. The inclusion of A_{π} changes the A_K value by 11%. We make use of the same resolution function $R_{sig}(t)$ for the $B^0 \rightarrow K^+ K^-$ events. The PDF for the continuum background events is $P_{q\bar{q}}(t) = (1+f_{q\bar{q}}) = 2f(f=2) e^{-\frac{1}{2}t^2} + (1-f)\delta(t)g$, where f is the fraction of the background with effective lifetime $\tau_{q\bar{q}}$, and δ is the Dirac delta function. We use $A_{q\bar{q}} = 0$ as a default. A fit to the sideband events yields $A_{q\bar{q}} = +0.01 \pm 0.01$ (-0.00 ± 0.01) for the data in Set I (II). This uncertainty in the background asymmetry is included in the systematic error for the S and A_{CP} measurement. The background PDF $P_{q\bar{q}}$ is convolved with a background resolution function $R_{q\bar{q}}$. All parameters in $P_{q\bar{q}}$ and $R_{q\bar{q}}$ are determined from sideband events.

We define a likelihood value for each (ith) event as a function of S and A_{CP} :

$$P_i = \prod_{k=1}^{Z+1} [f f^m P^q(t^0; w_1; S; A_{CP}) + f_K^m P_K^q(t^0; w_1) g R_{sig}(t_i - t^0) + f_{q\bar{q}}^m P_{q\bar{q}}(t_i - t^0)] d t^0 + f_{ol} P_{ol}(t_i); \quad (2)$$

Here, the probability functions f_k^m ($k = K$ or $q\bar{q}$) are determined on an event-by-event basis as functions of E and M_{bc} for each LR-tag bin ($m = 1, 12$). A small number of signal and background events that have large values of t is accommodated by the outlier PDF, P_{ol} , with fractional area f_{ol} . In the t , S and A_{CP} are the only free parameters and are determined by maximizing the likelihood function $L = \prod_i P_i$, where the product is over all the $B^0 \rightarrow K^+ K^-$ candidates.

The unbinned maximum likelihood fit to the 2,820 $B^0 \rightarrow K^+ K^-$ candidates containing 666 $+43$ signal events (1,486 B^0 tags and 1,334 \bar{B}^0 tags) yields $S = 0.67 \pm 0.16$ (stat) ± 0.06 (syst) and $A_{CP} = +0.56 \pm 0.12$ (stat) ± 0.06 (syst). The correlation between S and A_{CP} is $+0.09$. In this Letter, we quote the usual t errors from the likelihood functions, called the MINOS error, as statistical uncertainties [18]. Figures 2(a) and 2(b) show the t distributions for the 470 B^0 - and 414 \bar{B}^0 -tagged events in the subset of data with $LR > 0.86$. We define the raw asymmetry A_{CP} in each t bin by $A_{CP} = (N_+ - N_-)/(N_+ + N_-)$, where N_{\pm} is the number of observed candidates with $q = +1$ (-1). Figures 2(c) and 2(d) show the raw asymmetries for two regions of the flavor-tagging parameter.

Table I summarizes the systematic uncertainties on S and A_{CP} . The main contributions to the systematic error are due to the uncertainties in the vertex reconstruction (0.04 for S and $+0.03$ for A_{CP}) and event fraction (0.02 for S and 0.04 for A_{CP}), which includes the uncertainties in $A_{q\bar{q}}$ and final state radiation. We include the effect of tag-side interference [19] on S (-0.01) and A_{CP} ($+0.02$). Other sources of the systematic error are the

uncertainties in the wrong tag fraction, physics parameters (B^0 , m_d and A_K), resolution function, background shape, and bias. We add each contribution in quadrature to obtain the total systematic error.

We carry out a number of checks to validate our results. The B^0 lifetime is measured with $B^0 \rightarrow K^+ \pi^-$ candidates. The result is $\tau_{B^0} = 1.50 \pm 0.07$ ps, consistent with the world average value [20]. The CP fit to the sideband events yields no significant asymmetry. We check the measurement of A_S using a time-integrated fit and obtain $A_S = +0.52 \pm 0.14$, consistent with the time-dependent fit result. We also select $B^0 \rightarrow K^+ \pi^+$ candidate events with charged tracks positively identified as kaons that have a topology similar to the $B^0 \rightarrow K^+ \pi^-$ signal events. A fit to the 4,293 $B^0 \rightarrow K^+ \pi^-$ candidates (2,207 signal events) yields $S_K = +0.09 \pm 0.08$, consistent with zero, and $A_K = -0.06 \pm 0.06$, in agreement with the world average value [15]. With the K^+ sample, we determine $\tau_{B^0} = 1.51 \pm 0.04$ ps and $m_d = 0.46 \pm 0.03$ ps¹, which are also in agreement with the world average values [20].

To determine the statistical significance of our measurement, we apply the frequentist procedure described in Ref. [7] that takes into account both statistical and systematic errors. Figure 3 shows the resulting two-dimensional confidence regions in the S and A_S plane. The hypothesis of CP symmetry conservation, $S = A_S = 0$, is ruled out at a 99.999994% confidence level (CL), i.e., $1 \text{ CL} = 5.6 \times 10^{-8}$, equivalent to a 5.4 standard deviation for one-dimensional Gaussian errors. The case of no direct CP violation, $A_S = 0$, is also ruled out with a significance greater than 4.0 for any S value.

Figure 4 shows the E_T distributions for $B^0 \rightarrow K^+ \pi^-$ candidates with $LR > 0.86$ and $0.5 < r < 1.0$ for (a) $q = +1$ and (b) $q = -1$ subsets in the M_{bc} signal region. An unbinned two-dimensional maximum likelihood fit to the $q = +1$ ($q = -1$) subset yields 107 (13 (69 11)) K^+ , 42 (9 (43 9)) K^+ and 38 (1 (38 1)) continuum events in the signal box. The K^+ and continuum background yields are consistent between the two subsets as expected, while the K^+ yields are significantly different, thus large direct CP violation in $B^0 \rightarrow K^+ \pi^-$ decays is evident. These results also support the expectation from SU(3) symmetry that $A_S = 3 A_K$ [21].

We constrain the ratio of the magnitude of the penguin to tree amplitudes $P=T/j$ and a strong phase difference $\phi_P - \phi_T$ by adopting the notation of Ref. [22], where $\phi_P(\phi_T)$ is a strong phase of the penguin (tree) amplitude. By varying ϕ_2 in the range of 0° to 180° with $\phi_1 = 23.5^\circ \pm 1.6^\circ$ [15], we calculate a minimal CL of S and A_S in Fig. 3 for various $P=T/j$ and ϕ_2 . Figure 5 shows the CL contours of S and A_S for various $P=T/j$ and ϕ_2 . We find model-independent 95.4% confidence intervals of $P=T/j > 0.17$ and $180^\circ < \phi_2 < 4^\circ$.

To constrain ϕ_2 , we employ isospin relations [23] and the approach of Ref. [24] for the statistical treatment. We construct a χ^2 using the measured branching ratios of $B^0 \rightarrow K^+ \pi^-$, $B^0 \rightarrow \bar{K}^0 \pi^0$ and $B^0 \rightarrow \bar{K}^0 \pi^0$, and the direct CP asymmetry for $B^0 \rightarrow K^+ \pi^-$ [15] as well as our measured values of S and A_S taking into account their correlation. We minimize the χ^2 for various ϕ_2 values by varying the branching ratios and asymmetries by their errors and compute confidence levels. Figure 6 shows the obtained CL as a function of ϕ_2 . We find an allowed range for ϕ_2 at 95.4% CL of $0^\circ < \phi_2 < 19^\circ$ and $71^\circ < \phi_2 < 180^\circ$.

In summary, we have performed a new measurement of the CP-violating parameters in $B^0 \rightarrow K^+ \pi^-$ decays using a 253 fb⁻¹ data sample. We obtain $S = 0.67 \pm 0.16$ (stat) ± 0.06 (syst) and $A_S = +0.56 \pm 0.12$ (stat) ± 0.06 (syst). We rule out the CP-conserving case, $S = A_S = 0$, at the 5.4 level. We find compelling evidence for direct CP asymmetry with 4.0 standard deviations. The results complement the previous Belle measurement of the CP-

violating parameters as well as the earlier evidence for direct CP violation in $B^0 \rightarrow D^+ \pi^-$ decays [7].

We thank the KEKB group for the excellent operation of the accelerator, the KEK cryogenics group for the efficient operation of the solenoid, and the KEK computer group and the NII for valuable computing and Super-SINET network support. We acknowledge support from MEXT and JSPS (Japan); ARC and DEST (Australia); NSFC (contract No. 10175071, China); DST (India); the BK21 program of MOEHRD and the CHEP SRC program of KOSEF (Korea); KBN (contract No. 2P03B 01324, Poland); MIST (Russia); MESS (Slovenia); SNF (Switzerland); NSC and MOE (Taiwan); and DOE (USA).

- [1] M. Kobayashi and T. M. Takawa, *Prog. Theor. Phys.* **49**, 652 (1973).
- [2] Belle Collaboration, K. Abe et al., *Phys. Rev. Lett.* **87**, 091802 (2001); Belle Collaboration, K. Abe et al., *Phys. Rev. D* **66**, 032007 (2002); Belle Collaboration, K. Abe et al., *Phys. Rev. D* **66**, 071102 (2002).
- [3] Belle Collaboration, K. Abe et al., hep-ex/0408111, submitted to *Phys. Rev. D*.
- [4] BABAR Collaboration, B. Aubert et al., hep-ex/0408127, submitted to *Phys. Rev. Lett.*
- [5] Throughout this Letter, the inclusion of the charge conjugate mode decay is implied unless otherwise stated.
- [6] A.B. Carter and A.I. Sanda, *Phys. Rev. D* **23**, 1567 (1981); I.I. Bigi and A.I. Sanda, *Nucl. Phys. B* **193**, 85 (1981).
- [7] Belle Collaboration, K. Abe et al., *Phys. Rev. Lett.* **93**, 021601 (2004); see also Belle Collaboration, K. Abe et al., *Phys. Rev. D* **68**, 012001 (2003) for results based on a 78 fb^{-1} data sample. The results reported here supersede those of these two publications.
- [8] BABAR Collaboration, B. Aubert et al., hep-ex/0501071, submitted to *Phys. Rev. Lett.*
- [9] S. Kurokawa and E. Kikutani et al., *Nucl. Instr. and Meth. A* **499**, 1 (2003).
- [10] Belle Collaboration, A. Abashian et al., *Nucl. Instr. and Meth. A* **479**, 117 (2002).
- [11] Y. Ushiroda (Belle SVD2 Group), *Nucl. Instr. and Meth. A* **511**, 6 (2003).
- [12] H. Kakuno et al., *Nucl. Instr. and Meth. A* **533**, 516 (2004).
- [13] Belle Collaboration, K. Abe et al., hep-ex/0409049.
- [14] ARGUS Collaboration, H. Albrecht et al., *Phys. Lett. B* **241**, 278 (1990).
- [15] The Heavy Flavor Averaging Group (HFAG), hep-ex/0412073, <http://www.slac.stanford.edu/xorg/hfag> (2004).
- [16] H. Tajima et al., *Nucl. Instr. and Meth. A* **533**, 370 (2004).
- [17] Belle Collaboration, Y. Chao et al., *Phys. Rev. Lett.* **93**, 191802 (2004).
- [18] The rms values of the S and A distributions of MC pseudo-experiments were quoted as the statistical uncertainties in the previous publications [7]. With improved statistics, we find that MCNOS errors are approximately symmetric and agree well with the rms values (0.15 for S and 0.11 for A).
- [19] O. Long, M. Baak, R.N. Cahn, and D. Kirkby, *Phys. Rev. D* **68**, 034010 (2003).
- [20] Particle Data Group (S. Eidelman et al.), *Phys. Lett. B* **592**, 1 (2004), <http://pdg.lbl.gov>.
- [21] M. Gronau and J.L. Rosner, *Phys. Lett. B* **595**, 339 (2004), N.G. Deshpande and X.G. He, *Phys. Rev. Lett.* **75**, 1703 (1995).
- [22] M. Gronau and J.L. Rosner, *Phys. Rev. D* **65**, 093012 (2002).
- [23] M. Gronau and D. London, *Phys. Rev. Lett.* **65**, 3381 (1990).

[24] J. Charles et al., hep-ph/0406184.

TABLE I: Summary of the systematic uncertainties.

source	S	A
wrong tag fraction	0.01	0.01
physics parameters	< 0.01	0.01
resolution function	0.04	0.01
background t shape	< 0.01	< 0.01
event fraction	0.02	0.04
t bias	0.01	0.01
vertex	0.04 + 0.03	0.01
tag side interference	0.01 + 0.02	0.04
total	0.06	0.06

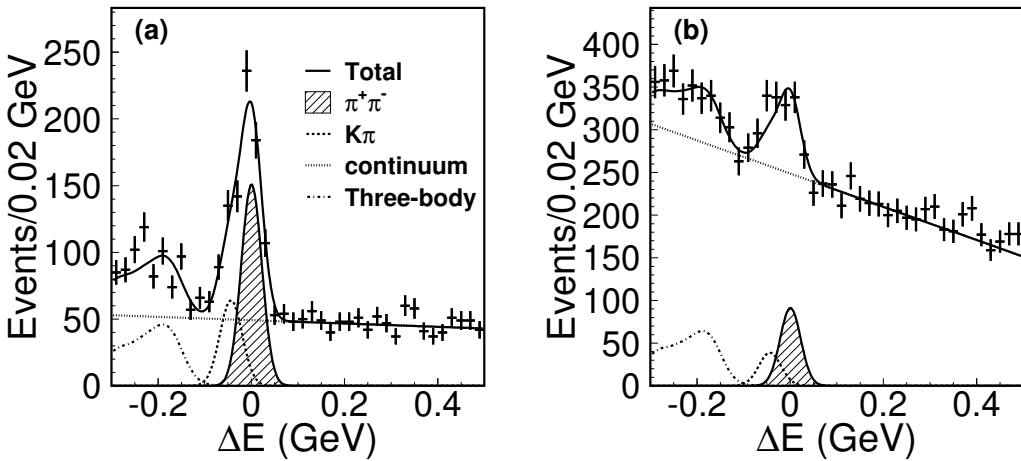


FIG. 1: The ΔE distributions in the M_{bc} signal region for $B^0 \rightarrow K^+ \pi^-$ candidates with (a) $LR > 0.86$ and (b) $LR < 0.86$. The sum of the signal and background functions is shown as a solid curve. The solid curve with hatched area represents the $B^0 \rightarrow K^+ \pi^-$ component, the dashed curve represents $K^+ \pi^-$ component, the dotted curve represents the continuum background, and the dot-dashed curve represents the three-body B decay background component.

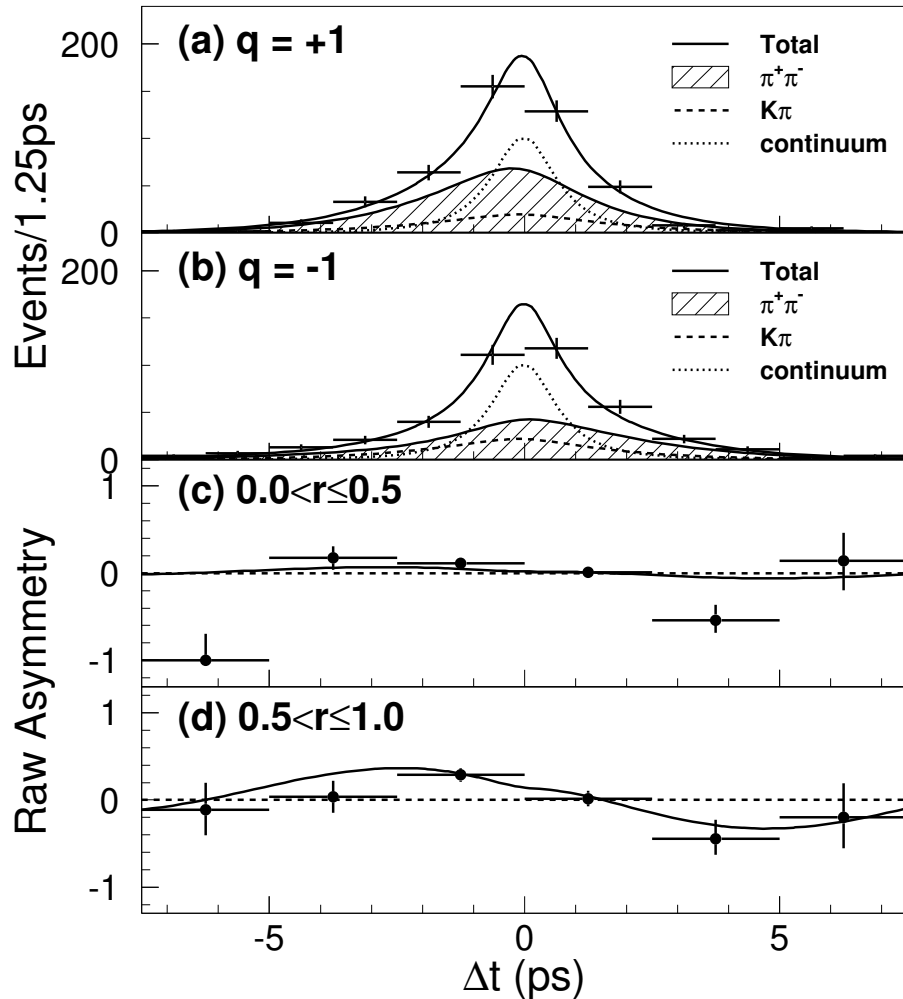


FIG. 2: The t distribution for the 884 $B^0 \rightarrow \pi^+ \pi^-$ candidates with $LR > 0.86$ in the signal region: (a) 470 candidates with $q = +1$, i.e., the f_{tag} is identified as a B^0 ; (b) 414 candidates with $q = -1$. Raw asymmetry, A_{CP} , in each t bin with (c) $0 < r \leq 0.5$ and (d) with $0.5 < r \leq 1.0$. The solid line shows the results of the unbinned maximum likelihood t to the t distribution of the 2,820 $B^0 \rightarrow \pi^+ \pi^-$ candidates.

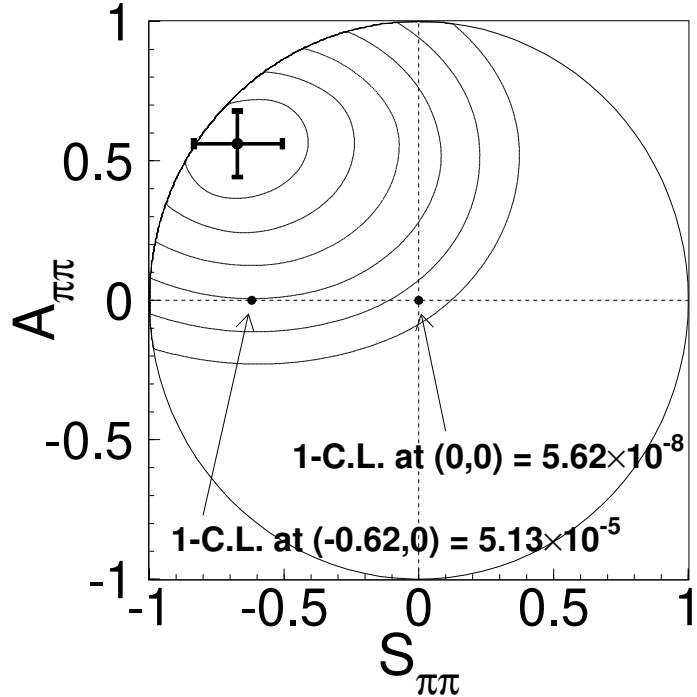


FIG .3: Con dence regions of $S_{\pi\pi}$ and $A_{\pi\pi}$. The curves show the contour for 1 C.L.:= 3:17 10^1 (1), $4:55 \times 10^2$ (2), $2:70 \times 10^3$ (3), $6:33 \times 10^5$ (4), $5:73 \times 10^7$ (5) and $1:97 \times 10^9$ (6) from inside to outside. The point with error bars is the $S_{\pi\pi}$ and $A_{\pi\pi}$ m easurement.

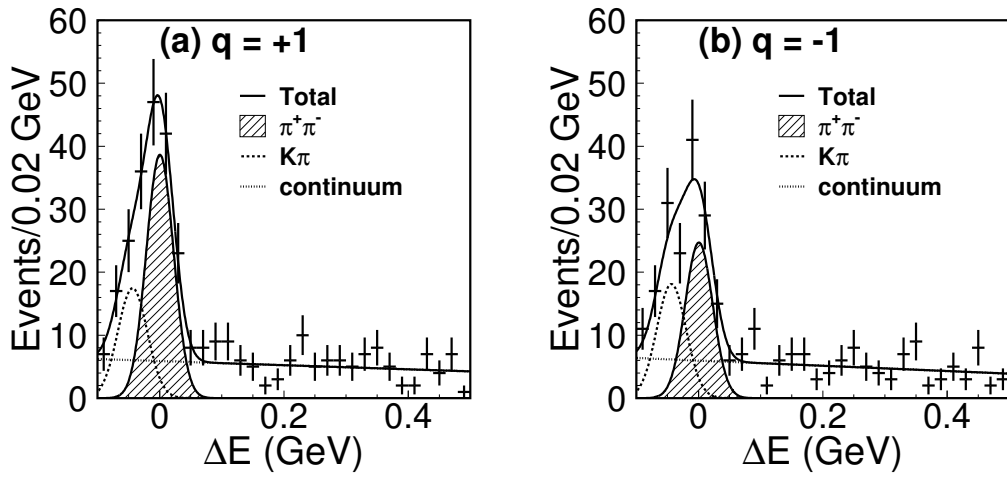


FIG .4: The ΔE distributions in the M_{bc} signal region for the $B^0 \rightarrow \pi^+ \pi^-$ candidates with $LR > 0.86$ and $0.5 < r < 1.0$ for (a) $q = +1$ and (b) $q = -1$. The sum of the signal and background components is shown as a solid curve. The solid curve with hatched area represents the $B^0 \rightarrow \pi^+ \pi^-$ component, the dashed curve represents $K^+ \pi^-$ component, and the dotted curve represents the continuum background.

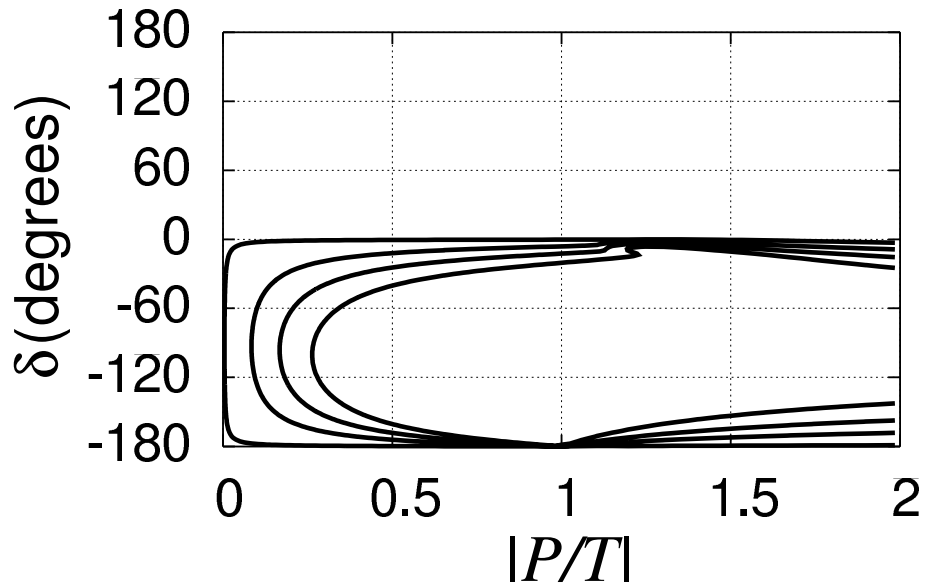


FIG. 5: Confidence levels of S and A for various $|P/T|$ and δ . The curves show the contour for $1 \text{ C.L.} = 3.17 \cdot 10^{-1}$ (1), $4.55 \cdot 10^{-2}$ (2), $2.70 \cdot 10^{-3}$ (3), and $6.33 \cdot 10^{-5}$ (4).

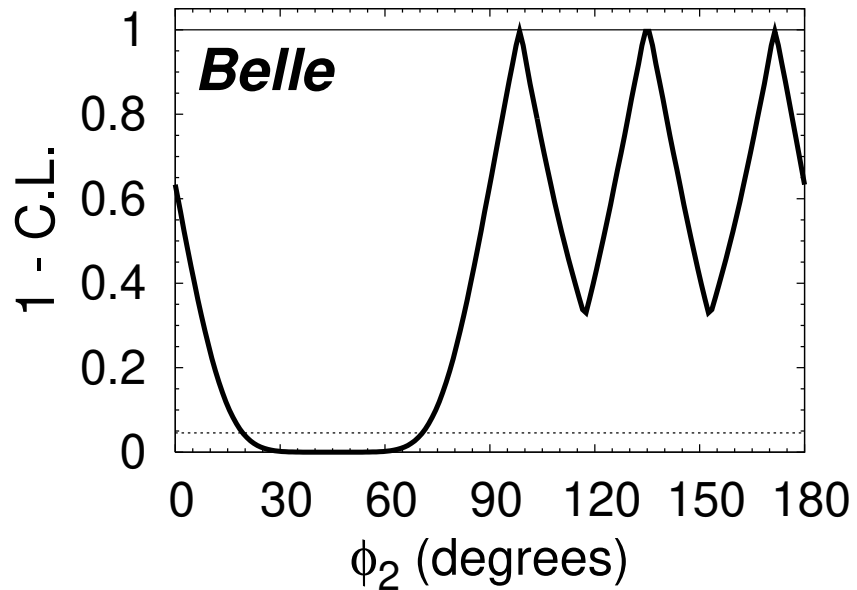


FIG. 6: Confidence level as a function of the CKM angle ϕ_2 obtained with an isospin analysis using Belle measurements of S and A .